The Egyptian Journal of Remote Sensing and Space Sciences (2014) 17, 159–170

HOSTED BY

ELSEVIER

National Authority for Remote Sensing and Space Sciences

The Egyptian Journal of Remote Sensing and Space Sciences

www.elsevier.com/locate/ejrs
www.sciencedirect.com

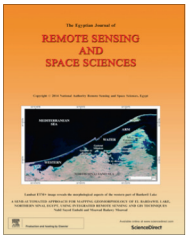

RESEARCH PAPER

The preparation of landslide map by Landslide Numerical Risk Factor (LNRF) model and Geographic Information System (GIS)

Ali Mohammadi Torkashvand [a,*], Akram Irani [b], Jaliledin Sorur [c]

[a] *Department of Soil Science, Rasht Branch, Islamic Azad University, Rasht, Iran*
[b] *Rasht Branch, Islamic Azad University, Rasht, Iran*
[c] *Department of Geography, Rasht Branch, Islamic Azad University, Rasht, Iran*

Received 23 January 2014; revised 27 July 2014; accepted 3 August 2014
Available online 5 September 2014

KEYWORDS

GIS;
Mass movements;
Sabalan;
Watershed

Abstract One of the risks to threaten mountainous areas is that hillslope instability caused damage to lands. One of the most dangerous instabilities is mass movement and much movement occurs due to slip. The aim of this study is zonation of landslide hazards in a basin of the Ardebil province, the eastern slopes of Sabalan, Iran. Geological and geomorphologic conditions, climate and type of land use have caused susceptibility of this watershed to landslides. Firstly, maps of the main factors affecting landslide occurrence including slope, distance from faults, lithology, elevation and precipitation were prepared and digitized. Then, by using interpretation of aerial photos and satellite images and field views, the ground truth map of landslides was prepared. Each basic layer (factor) and landslide map were integrated to compute the numeric value of each factor with the help of a Landslide Numerical Risk Factor (LNRF) model and landslide occurrence percent obtained in different units from each of the maps. Finally, with overlapping different data layers, a landslide hazard zonation map was prepared. Results showed that 67.85% of the basin has high instability, 7.76% moderate instability and 24.39% low instability.

1. Introduction

Soil erosion is defined as a "physical process with considerable variation globally in its severity and frequency" which is also dependent on various social, economic and political factors besides climatic factors (Mohamed et al., 2013). Massive erosion as a kind of erosion feature is the huge voluminous movement of soil or rock mass or a combinination of them down the slope by the gravitational force. In fact, this erosion occurs when the force resulting from the weight of the material is

* Corresponding author. Tel.: +98 131 4247058; fax: +98 131 4223621.
E-mail addresses: m.torkashvand54@yahoo.com, torkashvand@iaurasht.ac.ir (A.M. Torkashvand).
Peer review under responsibility of National Authority for Remote Sensing and Space Sciences.

1110-9823 © 2014 Production and hosting by Elsevier B.V. on behalf of National Authority for Remote Sensing and Space Sciences.
http://dx.doi.org/10.1016/j.ejrs.2014.08.001

higher than the resistance force from soil shear force. Usually, massive erosion is aligned with natural erosion, but human intervention intensifies this by operations such as mine excavation, road construction and destruction of forest vegetation (deforesting). Massive movements generally occur in three forms including soil mass slide (in steep slopes), landslide and mud flow. Landslide is major erosion which sometimes causes life loss, such as a huge sliding soil mass during an earthquake whichburies adjacent residential areas. Any factor that causes low soil resistance against shear forces, leads to increased landslides (Refahi, 2000). Bouma and Imeson (2000) after rainfall simulation experiments in the area of Petrer, southeast of Spain, concluded that runoff, infiltration and soil chemical and mineralogical characteristics affect mass movements. Also, they concluded that high soil infiltration capacity caused soil instability and increased risk of massive erosion. Landslides are increased by massive erosion too. Among the factors creating landslides, underground erosion increases soil mass instability (Furuya et al., 1999). Sassa (1984) studied landslide movement and groundwater levels in Zentokoy, Japan, and suggested that landslides have been created by groundwater erosion.

In different countries, it is serious issue to achieve solutions, suitable methods to inhibit; control and mitigation of soil erosion, mass movements, decreasing damage caused by natural disasters and the principles of planning in using natural environments. Rasmy et al. (2010) presented the development of a system dynamic model to simulate and analyze the potential future state of desertification in Egypt. Haq et al. (2012) developed techniques for mapping flood extent and assessing flood damages which can be served as a guideline for RS and GIS operations to improve the efficiency of flood disaster monitoring and management. In order to prioritize the area for hazard-mitigation efforts, it is beneficial to have a landslide hazard map to rank the area based on actual and/or potential threat of slides in future (Anbalagan, 1992). Landslide hazard assessment is being carried out using qualitative or quantitative approaches (Aleotti and Chowdhury, 1999). The qualitative methods essentially depend on expert opinion in dividing an area into different zones of varying landslide susceptibility. Using an inventory of existing landslides, the expert can assess hazards of the area by identifying regions of similar geological and geomorphological conditions (Ayalew and Yamagishi, 2005). Gupta et al. (1999) and Saha et al. (2002) used the parameter-weighting method for landslide hazard zonation mapping in part of the Bhagirathi valley of Garhwal Himalaya. NRSA (2001) adopted the Analytical Hierarchy Process methodology for preparing landslide hazard zonation maps along the corridors of the major pilgrimage routes in Uttarakhand, Uttar Pradesh and Himachal Pradesh Himalaya.

Busoni et al. (1995) studied a basin of Eurasia in Italy and according to the relationship between land form, slope, hydrographic network model, river bed, erosion features, vegetation and land use, culture management systems, diagnosed 17 land units and 46 types of land. Multivariate analysis of above parameters showed that the five variables of slope, hydrographic network patterns, erosion features, mass movement and land use are sufficient to determine erosion risk and mass

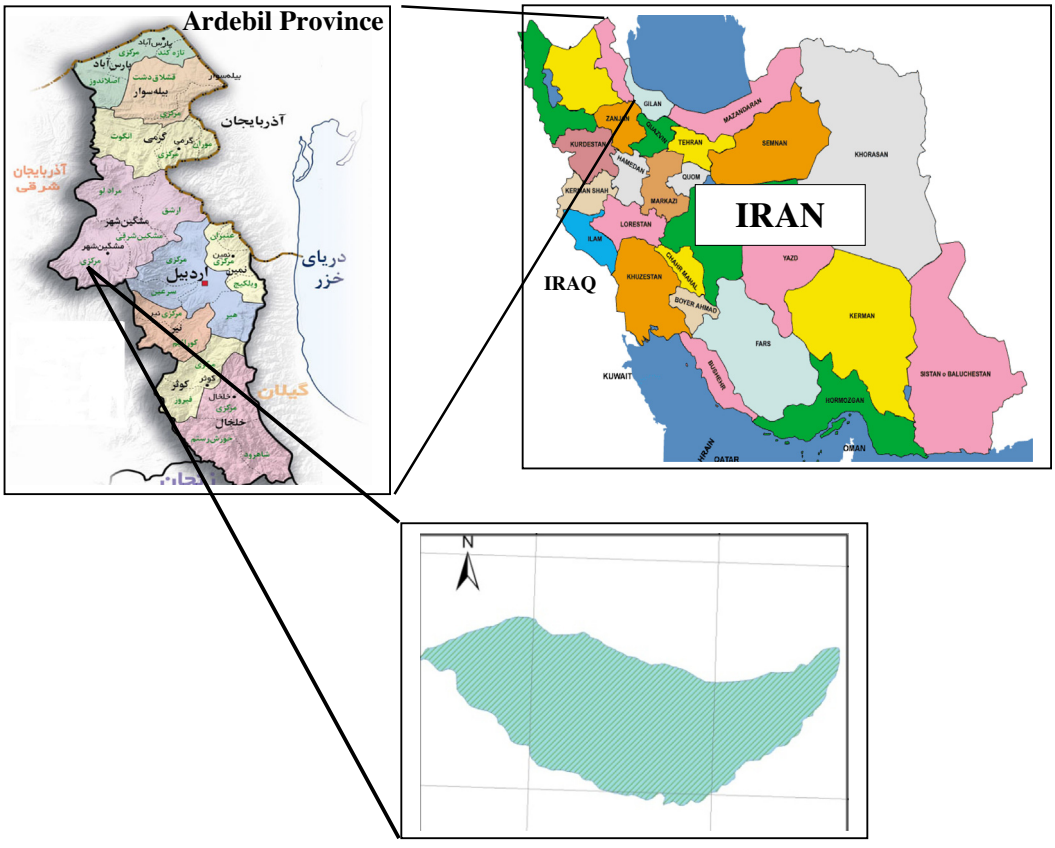

Figure 1 The location of studying basin.

movement coefficient. In the Western Ghats in India, GIS and RS techniques were used for finding the landslide prone areas (Najarjan et al., 1998) found that using this technique was more successful than previous methods.

In order to determine zoning of landslide risk, Hassanzadeh (2000) used the multiple regression method and GIS techniques using four data layers of lithology, slope angle, rainfall and the land use and achieved successful results. Esmali and Ahmadi (2003) used GIS to prepare the landslide map. They determined landslide prone areas on aerial photographs and in the next step, these areas were controlled by field views and those areas that were not likely to slip, were removed. Landslide maps were overlapped on each of the layers of lithology, slope, usage, linear factor (rivers and roads), precipitation classes, elevation classes and erosion features and the landslide number was calculated in each unit. Each unit was evaluated in accordance with landslide number from 0 to 100. The weight of each factor associated with the risk of erosion in the region was calculated and finally they prepared the landslide hazard map in five classes of very low to very high according to the AHP (Analytical Hierarchy process) method.

The efficiency of two methods of landslide zoning including the revised Nilson and Taiwan method and Association of Engineering Geology was investigated by Habibi et al. (2005) through the GIS in Kan and Solqhan basin. They prepared a hazard landslide zonation map by using two cited methods and the map accuracy was calculated as compared to the ground truth map. Their results showed that the revised Nilsson landslide hazard map had 96.5% compliance with the ground truth map of the landslide, whereas the slide hazard zonation map of the Geological Society of Taiwan had 78.4% compliance. Gupta and Joshi (1990) presented a model in zoning landslide hazard using GIS called Landslide Numerical Risk Factor (LNRF) model that is a suitable model especially in the mountainous regions. Therefore, the purpose of this study is zoning of landslide by the aid of the LNRF model in a basin of Sabalan in the North East of Iran that is a mountainous basin.

Table 1 The units weight base on the LNRF model.

LNRF	Weight
0.67 >	0
0.67–1.33	1
1.33 <	2

2. Materials and methods

The studied area is in the East of the Sabalan volcanic mass located between 38°30′ and 38°22′ northern latitude and 42°16′ and 41°54′ eastern longitude (Fig. 1). The highest elevation in the west of the basin is 3800 m and the lowest elevation is in an outlet at 1340 m. So, it is a basin that has longitudinal strain. The basin has a deep and steep-sided valley. The amount of annual precipitation is 431.3 mm (Sabagh, 2009).

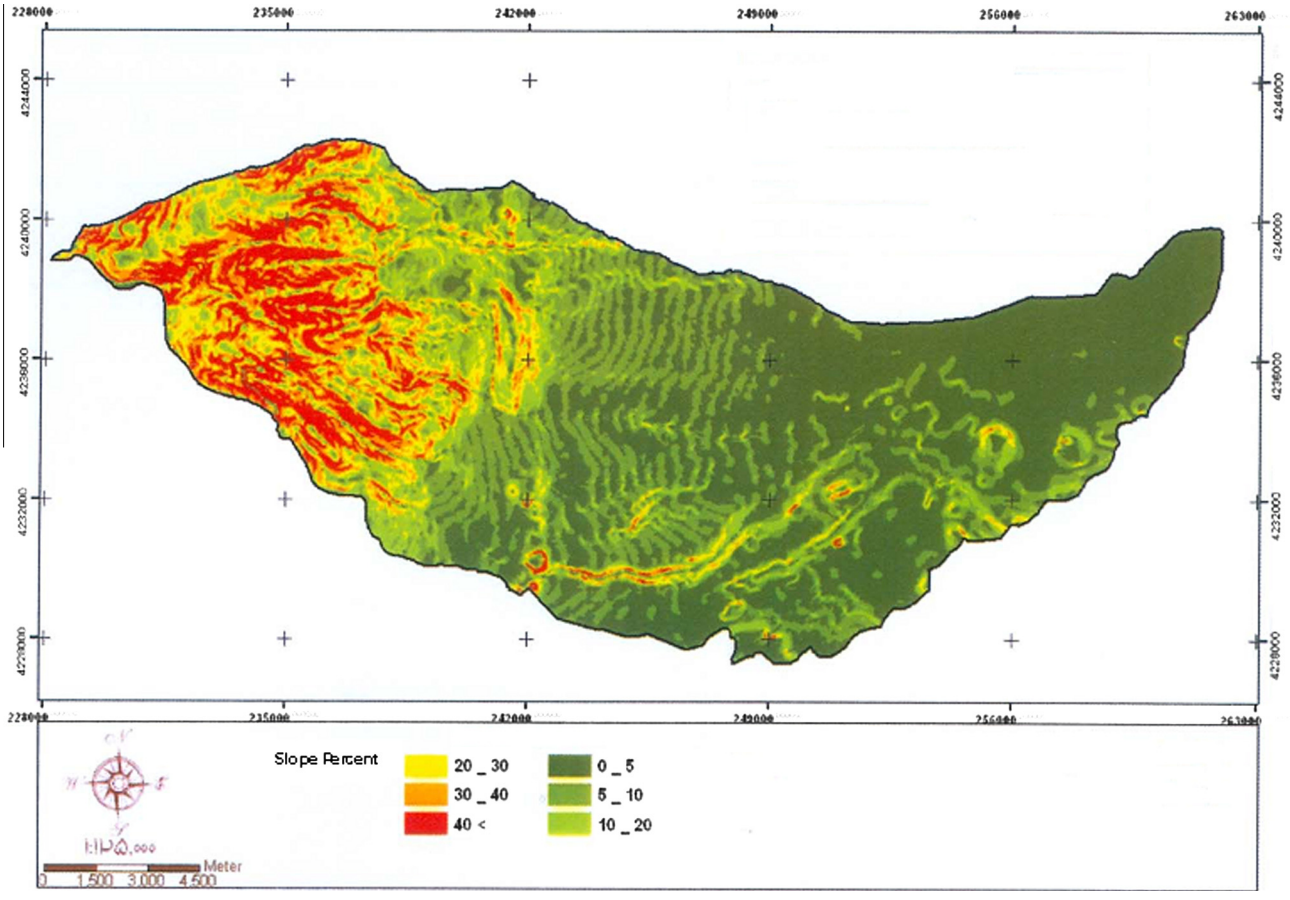

Figure 2 The slope layer of the basin.

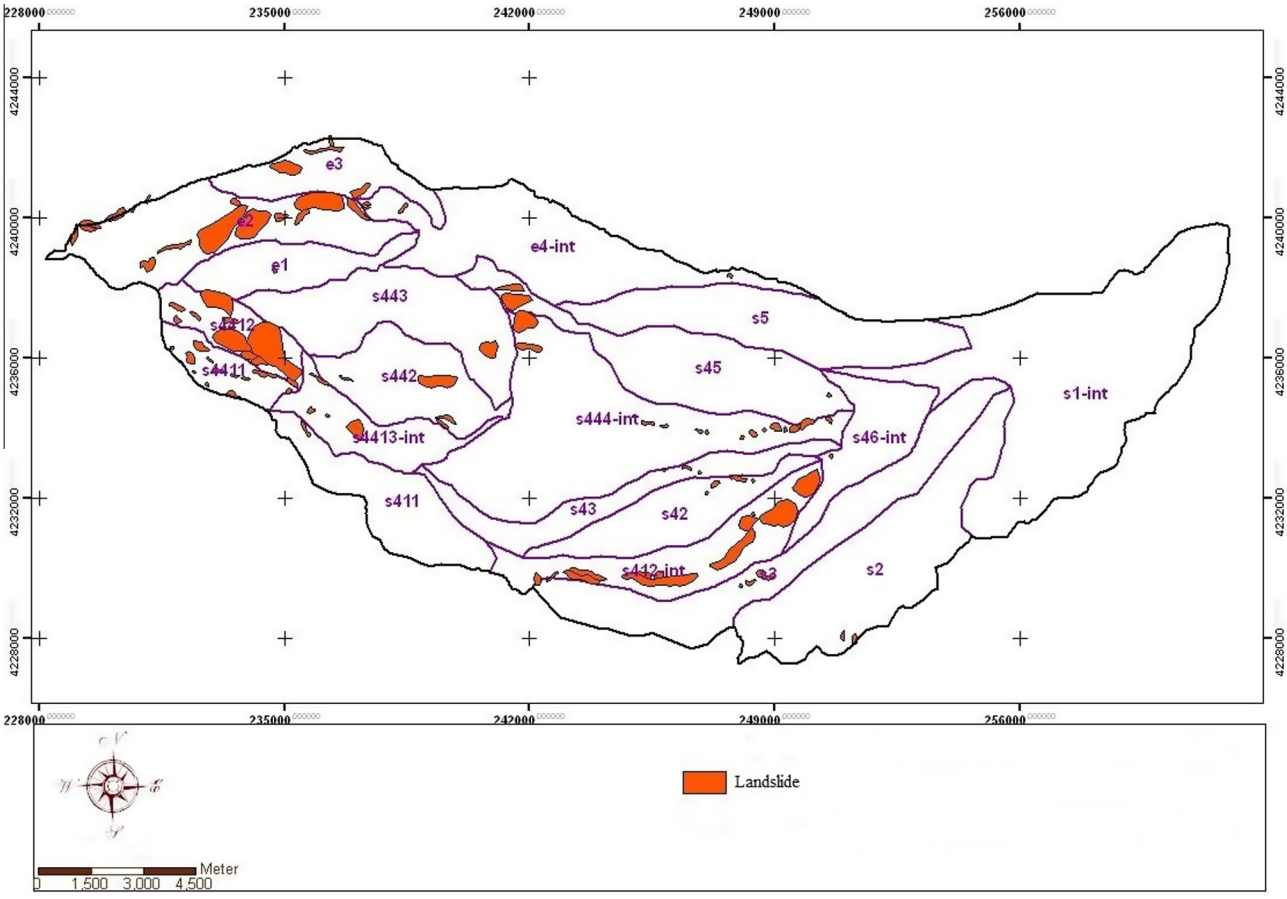

Figure 3 Landslide distribution (ground truth of landslide) in the basin (s443, s442, s1-int, …. are codes related to hydrological units).

Table 2 The results of integration of landslide layer and lithology layer.

Row	Lithology	Area unit		Land slide area		LNRF	Weight	Instability
		Hectare	Percent	Hectare	Percent			
1	Porphyritic, Trachyandesite Trachyte	669.1	2.53	99.4	1.18	9.05	1	Medium
2	Alluvium deposits	681.5	2.57	23.4	0.28	2.13	0	Low
3	Porphyritic Andesitic Basalt Andesitic lava	6411.6	24.20	552.5	6.5	50.31	2	High
4	Yang terraces and high level piedmont alluvium plain deposits	2716.0	10.25	72.0	0.85	6.56	0	Low
5	Conglomerate with some tuff volcano ash and lahars	10637.2	40.14	234.5	2.8	21.35	2	High
6	Tuffit lahar	250.0	0.94	0.0	0	0.00	0	Low
7	Silt	862.0	3.25	0.6	0.007	0.05	0	Low
8	Glacial moraine	97.5	0.37	6.0	0.07	0.54	0	Low
9	Andesitic basalt – Trachy basalt –Basalt trachyte	1057.3	3.99	101.2	1.2	9.22	1	Medium
10	Travertine	985.1	3.72	5.3	0.06	0.48	0	Low
11	Old terraces and high level piedmont lava	550.0	2.08	0.13	0.0015	0.01	0	Low
12	Tephra with vesicular basaltic fragments	1569.1	5.92	0.0	0	0.00	0	Low
13	Irregular river bed	10.7	0.04	3.1	0	0.28	0	Low
	Total	26497.2	100	1098.2	1.18	100		

The basin is on an elevated plateau in the west of Alborz–Azerbaijan tectonic zones that mostly has been covered with volcanic rocks (Khayyam, 1993). The type of formations and lithology are factors for the occurrence of mass movements. According to the geological map the major lithology of this basin is conglomerate along with Lahar, volcanic ashes, andesite, basalt and truck basalt. Soil moisture and temperature regimes are Xeric and Mesic, respectively. Soils are located in alfisol and inceptisol orders. The climate of the basin base in the De Martonne method is semi-arid and highly cold. According to the studies of Saber (2009), much basin has vegetation cover and only part of the mountainous lands has a rock outcrop without soil and vegetation cover, which includes about 9.83% of the total watershed area.

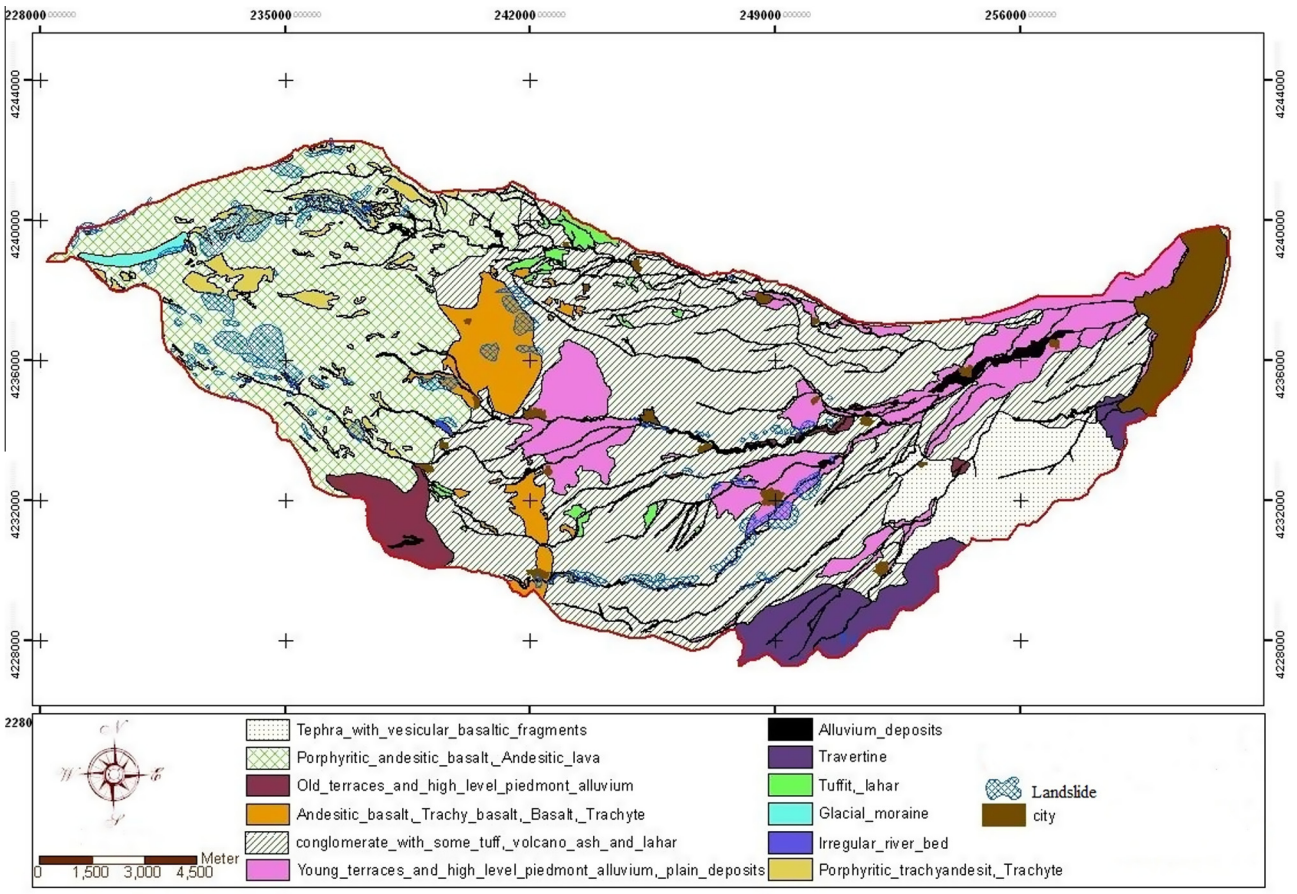

Figure 4 The map obtained from the overlay of landslides on the Lithology map.

Various natural and human factors are involved in the occurrence of landslide, so in this study, the most important factors including lithology, distance from the fault, elevation, rainfall, land use and slope, were selected and by using Landslide Numerical Risk Factor (LNRF) model, weighted value for every phenomenon was determined. Fig. 2 shows the slope layer of the basin. In this method, which is called the credibility factor of landslide risk, by using the occurred slip surface in a unit than mean occurred slip in the whole unit, the index is prepared. This model is calculated from Eq. (1):

$$\mathrm{LNRF} = \mathrm{A}/\mathrm{E} \tag{1}$$

A: landslide area in every unit,

E: mean area of landslide in the whole unit.

In Eq. (1), the weight of each homogeneous unit is estimated and weighted maps and related tables were prepared; and LNRF in every homogeneous unit in three categories of low instability (0), medium (1) and high (2) is calculated (Table 1). Finally, by algebraic addition of weighted maps, a zoning map of the hillslope instability was prepared.

Slips location with the help of aerial photos and field studies was identified and the ground truth map of the landslide was prepared (Fig. 3). By a GIS (ArcGIS9.2 software), digitized layers of lithology, slope, distance from the fault, precipitation, land use, elevation, and lithology were prepared to combine with the landslide layer. Then, by using the LNRF model, the weight of every unit was calculated and weighted maps were prepared. By the integration of weighted maps, a zoning map of vulnerability risk to landslide in three categories including high instability, medium instability, and low instability, was prepared.

3. Results

3.1. Lithology

Table 2 shows the results of landslide integration and lithology layers. Fig. 4 shows the overlay of the landslide layer on the lithology layer. The most landslide prone areas have occurred in porphyritic andesitic, basalt andesitic lava and then in the conglomerate with some tuff volcano ash and lahars. The results showed that 50.31% of slips have occurred in andesite and basalt lavas. This can be due to the existence of large basement faults in this region. The existence of slopes over 20% in this region can be another reason for the occurrence of landslides.

3.2. Fault distance

In the basin, tectonic movement intensifies the occurrence of mass movements. As can be seen in Table 3 and Fig. 5, the highest landslides have occurred with 39.18% of the total watershed area at a distance of less than 500 m from the main rock, its effect on the occurrence of slope movement is reduced and the instability of slopes is also lower.

Table 3 The results of integration of landslide layer and distance of fault layer.

Row	Distance of fault (m)	Area unit		Landslide area		LNRF	Weight	Instability
		Hectare	Percent	Hectare	Percent			
1	0–500	4716.4	17.8	437.1	39.18	10.19	2	High
2	500–1000	4371.4	16.5	48.3	4.33	1.12	1	Medium
3	1000–1500	3678.6	13.88	116.4	10.43	2.71	2	High
4	1500–2000	2398.7	9.05	92.7	8.31	2.16	2	High
5	2000–2500	1847	6.97	107	9.59	2.49	2	High
6	2500–3000	1710.6	6.46	94.8	8.5	2.21	2	High
7	3000–3500	1390.7	5.25	75.3	6.75	1.76	2	High
8	3500–4000	1191.7	4.5	55.4	4.97	1.29	1	Medium
9	4000–4500	988.7	3.73	29.3	2.63	0.68	0	Low
10	4500–5000	672.8	2.54	21.6	1.94	0.5	0	Low
11	5000–5500	498.4	1.88	11.6	1.04	0.27	0	Low
12	5500–6000	419.9	1.58	6	0.54	0.14	0	Low
13	6000–6500	385.2	1.45	10.4	0.93	0.24	0	Low
14	6500–7000	343.4	1.3	9.6	0.86	0.22	0	Low
15	7000–7500	298.8	1.13	0	0	0	0	0
16	7500–8000	263.6	0.99	0	0	0	0	0
17	8000–8500	204.7	0.77	0	0	0	0	0
18	8500–9000	191.4	0.72	0	0	0	0	0
19	9000–9500	189.1	0.71	0	0	0	0	0
20	9500–10,000	169.7	0.64	0	0	0	0	0
21	10,000–10,500	148.8	0.56	0	0	0	0	0
22	10,500–11,000	122.9	0.46	0	0	0	0	0
23	11,000–11,500	118.3	0.45	0	0	0	0	0
24	11,500–12,000	102.9	0.39	0	0	0	0	0
25	12000–12500	62.9	0.24	0	0	0	0	0
26	12500–13000	10.6	0.04	0	0	0	0	0
	Total	26497.2	100	1115.6	100			

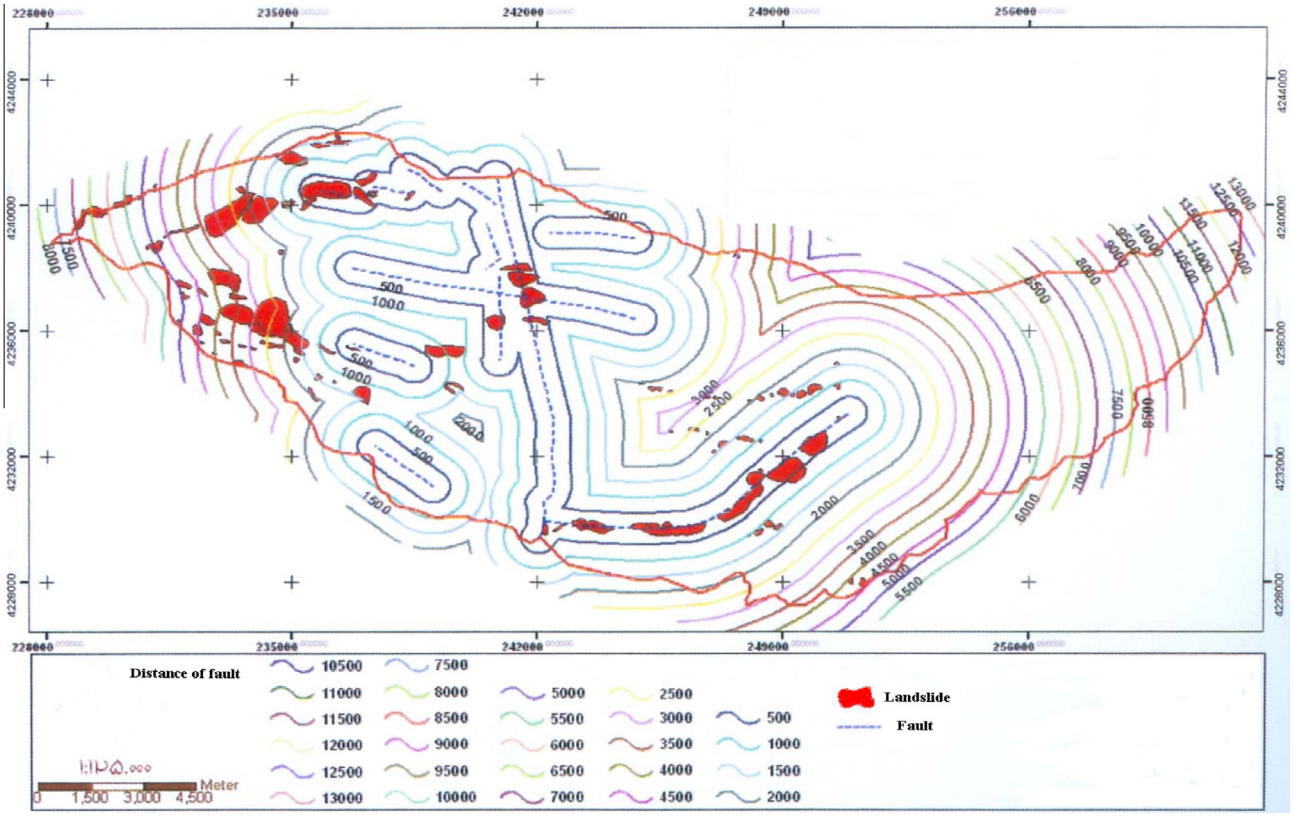

Figure 5 The landslides overlay on distance of the fault map.

Table 4 The results of integration of landslide layer and slope layer.

Row	Slope (%)	Area unit		Landslide area		LNRF	Weight	Instability
		Hectare	Percent	Hectare	Percent			
1	0–5	10344.8	39.04	81	7.38	0.44	0	Low
2	10-May	6045.2	22.81	77	7.01	0.42	0	Low
3	20-Oct	3659.7	13.81	184.5	16.8	1	1	Medium
4	20–30	2498.5	9.43	248.3	22.61	1.36	2	High
5	30–40	1925.7	7.27	227	20.67	1.24	1	Medium
6	40 <	2023.3	7.64	280.3	25.53	1.53	2	High
	Total	26497.2	100	1098.2	100			

3.3. Slope

In the basin, according to carried out studies, 43.28% of landslides on 40–20% slopes and 25.53% of movements occurred in a slope of more than 40% (Table 4). Although areas with slopes above 40% occupied a few of the areas (7.64), but one can see that the most slips occurred on this slope.

3.4. Elevation levels

Table 5 and Fig. 6 show a combination of landslide layer and elevation level layer. Elevation levels of the basin vary from 1329 m in the outlet basin to 3812.7 m in the altitude of the basin. Basin elevation classes are divided into 13 categories and the mean height of the basin is estimated by 1887.13 m. The most frequent height is related to height classes of 1500–1700 m (27.12%) and the least frequent height is related to the height classes of 3700–3812.7. Most movements also have occurred in the height range of 1500–1700 m.

3.5. Rainfall rate

In the basin, the average annual precipitation is 431.3 mm. Studies of the mean monthly rainfall at selected stations in the basin showed that the highest rainfall occurs in the months of April and May and the lowest rainfall occurs in August. Precipitation will fall from mid-November until March, as snow. To evaluate the relationship between rainfall and mass movements, the map of the basin rainfall was prepared from the statistics of rain gauge stations around the studied basin into 13 co-rain levels (Table 6). Table 6 shows that the highest rainfall class with 32.82% area is 300–450 mm class and the greatest landslide also occurred in this same class of rainfall. Fig. 7 shows the overlay of the rainfall layer on landslide layer.

3.6. Land use

Fig. 8 shows the overlay of the land use layer on the landslide layer. Effects of land use on slope stability are dependant on local conditions, soil depth, slope, type of plants, rocks condition and weather. Sometimes land use is the cause of stability and in some conditions, it stimulates hillslope instability. Plant roots absorb part of the underground water to increase slope stability due to drying of soil in slopes. In some conditions the water penetration to the lower layers of soil causes soil moistening, fluidity and soil mass movement on the slope. In this research, regional land uses were rangeland, forest and cultivated lands of which the results of integration of the landslide layer with land use layer is seen in Table 7.

4. Discussion

Results showed that the potential of mass movement is high in the basin. Hillslope morphology has a very large effect on the landslide occurrences (Dai and Lee, 2002). Slope is considered as the important factor and the main reason of slope shakes (Haeri and Samiei, 1996). Most instability occurred in the slope more than twenty percent. In slopes 0–10%, there was

Table 5 The results of integration of landslide layer and elevation level layer.

Row	Height classes (m)	Area unit		Landslides area		LNRF	Weight	Instability
		Hectare	Percent	Hectare	Percent			
1	1339–1500	6089.5	22.98	45.3	4.12	0.5	0	Low
2	1500–1700	7184.7	27.12	234.5	21.36	2.65	2	High
3	1700–1900	4004.0	15.11	39.1	3.56	0.43	0	Low
4	1900–2100	2420.9	9.14	129.7	11.81	1.41	2	High
5	2100–2300	1658.0	6.26	30.4	2.76	0.33	0	Low
6	2300–2500	1445.0	5.45	86.0	7.83	0.93	0	Low
7	2500–2700	1086.0	4.10	130.6	11.89	1.42	2	High
8	2700–2900	815.0	3.08	170.8	15.55	1.86	2	High
9	2900–3100	656.7	2.48	125.0	11.38	1.36	2	High
10	3100–3300	489.2	1.85	66.0	6.01	0.72	0	Low
11	3300–3500	414.4	1.56	22.7	2.06	0.24	0	Low
12	3500–3700	199.0	0.75	8.2	0.75	0.09	0	Low
13	3700–3812.7	35.1	0.13	10.0	0.91	0.1	0	Low
	Total	26497.2	100	1098.19	100			

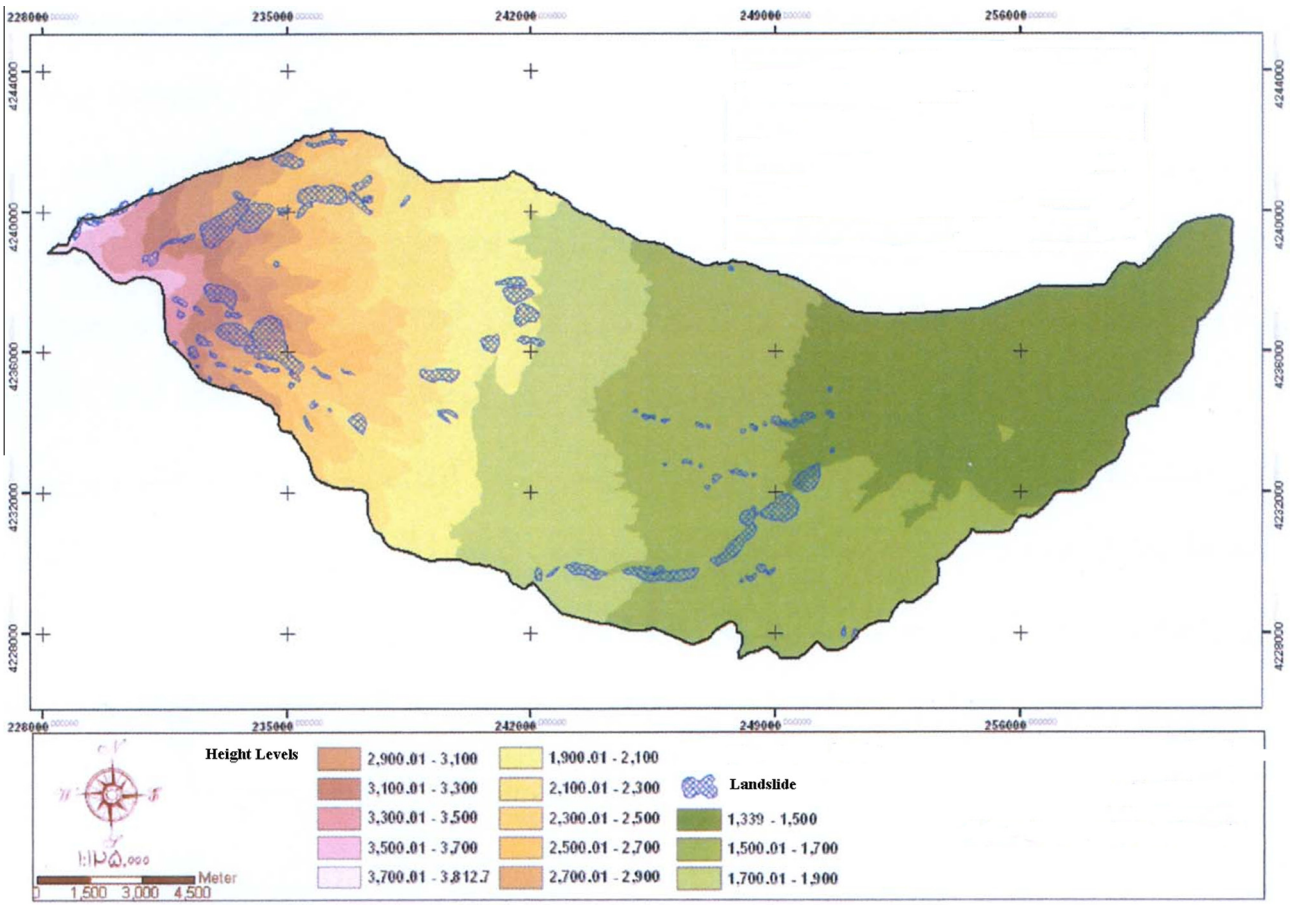

Figure 6 The landslides overlay on height (elevation) level map (hypsometric map).

Table 6 The results of integration of landslide layers and rainfall layer.

Row	Precipitation levels (mm)	Area unit		Landslide area		LNRF	Weight	Instability
		Hectare	Percent	Hectare	Percent			
1	264.8–300	1564.5	5.90	0.0	0.00	0	0	Low
2	300–450	8695.9	32.82	200.0	18.21	2.37	2	High
3	450–600	5466.8	20.63	112.8	10.27	1.33	2	High
4	600–750	3277.0	12.37	105.8	9.63	1.25	1	Medium
5	750–900	1905.5	7.19	55.0	5.01	0.65	0	Low
6	900–1050	1532.6	5.78	51.7	4.71	0.61	0	Low
7	1050–1200	1281.3	4.84	143.2	13.04	1.70	2	High
8	1200–1350	887.9	3.35	180.9	16.47	2.14	2	High
9	1350–1500	713.4	2.69	136.1	12.39	1.61	2	High
10	1500–1650	522.8	1.97	71.5	6.51	0.84	0	Low
11	1650–1800	434.3	1.64	22.7	2.07	0.27	0	Low
12	1800–1950	191.9	0.72	10.5	0.96	0.12	0	Low
13	1950–2012.5	23.2	0.09	8.0	0.73	0.09	0	Low
	Total	26497.2	100		100			

the minimum land sliding. The slopes more than 40% were seen in the low area of the basin (7.64%), but most slip occurred on these slopes. Saha et al. (2002) in zonation of landslide hazards, introduced slope more than 45% as the instability factor.

Height above the sea level also infers fluctuations and climatic changes. Elevation changes have an important influence on the three factors of temperature, precipitation and humidity (Khezri et al., 2006). In the heights of 1700–1500 m, the highest landslides (21.36%) had occurred. The gender of rocks in this range of heights is conglomerate and tuff that, due to high porosity and permeability, are more prone to slip. Shadfar et al. (2005) investigated the zoning of landslides in the basin of Laktrashan in Tonekabon by using the LNRF model. Their

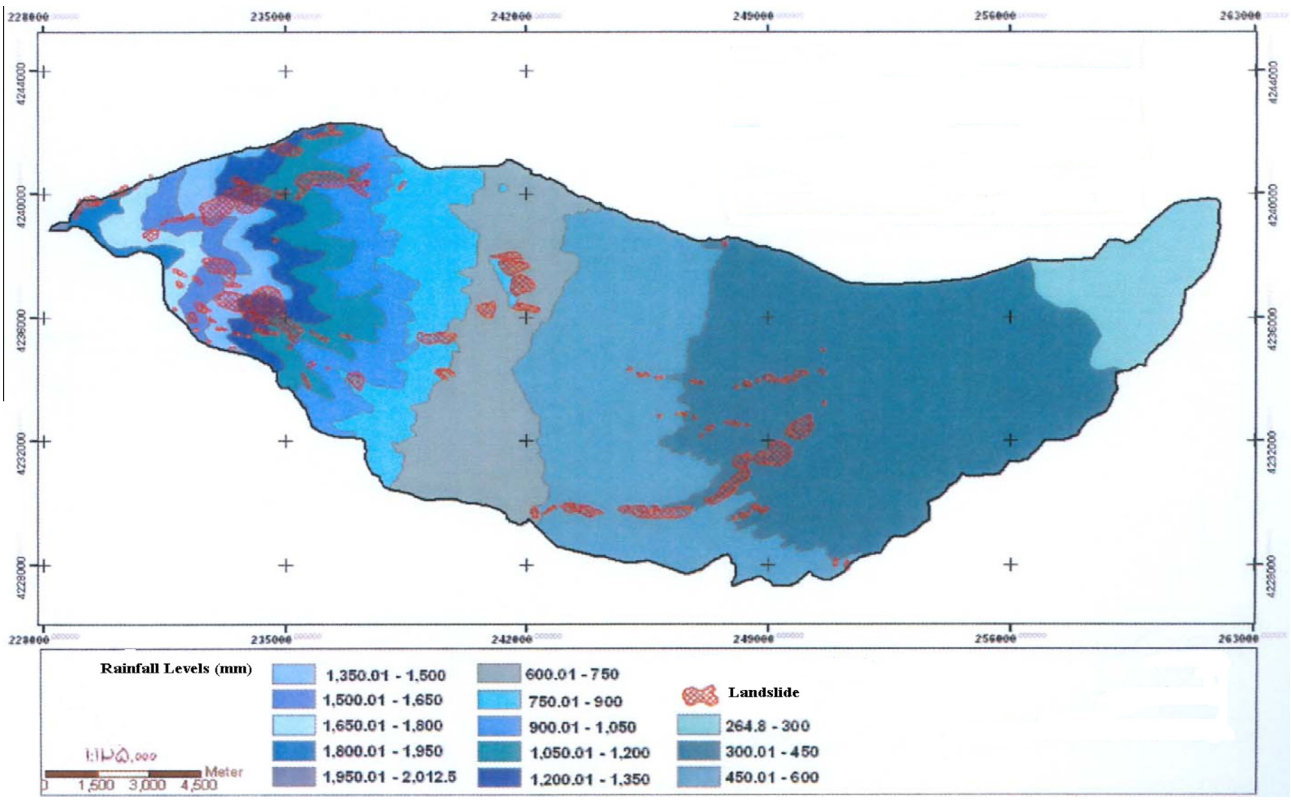

Figure 7 The landslides overlay on rainfall level map.

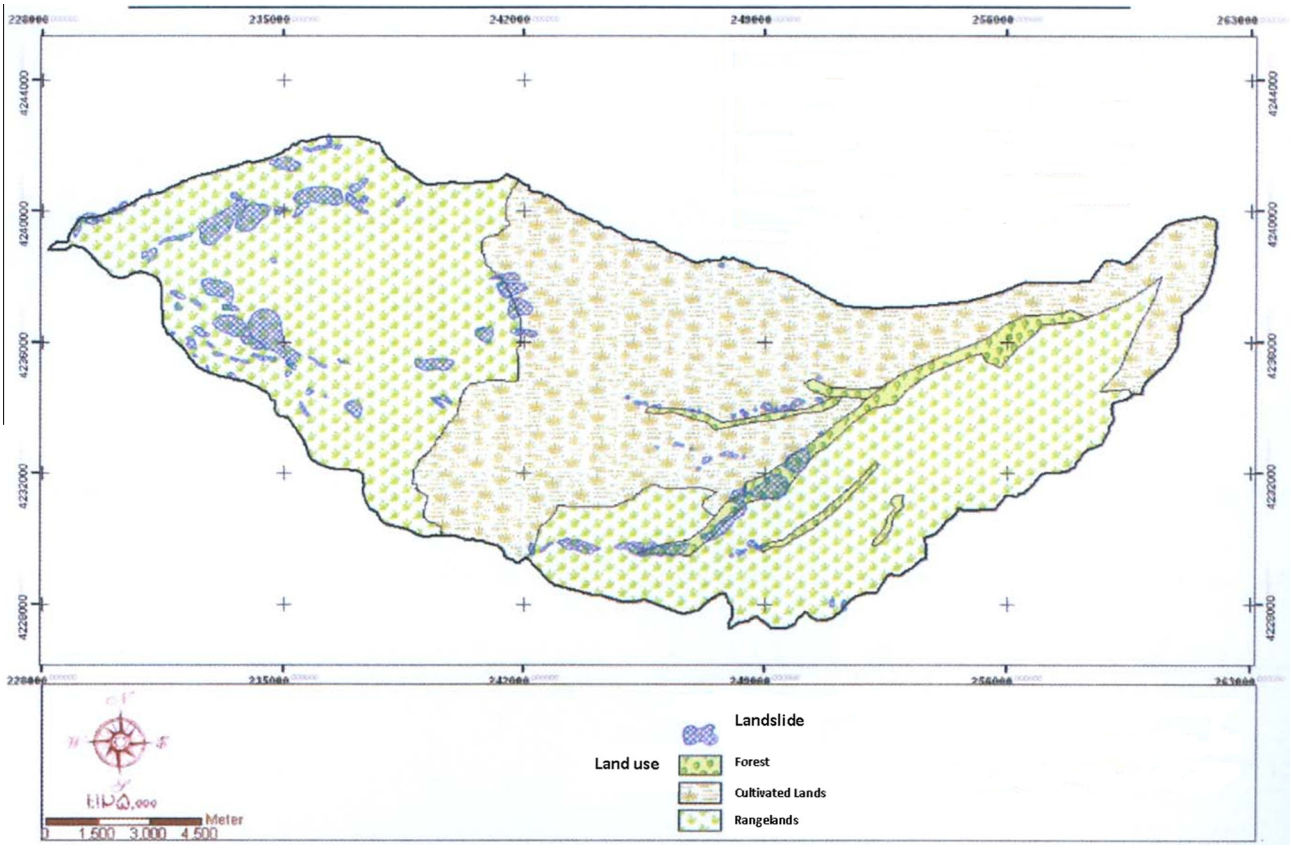

Figure 8 The landslides overlay on Land use map.

Table 7 The results of integration of landslide layers and land use layer.

Row	Land use	Area unit		Landslides area		LNRF	Weight	Instability
		Hectare	Percent	Hectare	Percent			
1	Grassland	15249.5	57.55	835.28	76.06	2.28	2	High
2	Forest	945.4	3.57	147.45	13.43	0.4	0	Low
3	Agriculture	10302.3	38.88	115.46	10.51	0.32	0	Low
	Total	26497.2	100	1098.2	100			

Table 8 The area of foothills instability in the basin.

Row	Instability	Area per category (ha)	Ratio to basin area (%)
1	Low	6463.6	24.39
2	Medium	2055.2	7.76
3	High	17978.4	67.85
	Total	26497.2	100

results showed that LNRF models have very good efficiency in zoning landslides, especially in semi-humid and humid areas. The results also showed that lithology factors (clay, silt with layers of sandstone), slope (30–40%) and the northwestern slope direction due to the receiving of higher humidity from the Caspian Sea had the most effect on the occurrence of the basin landslides.

Precipitation intensity and its duration have a major role in the occurrence of landslides, which of course depends on factors such as topography and geological structure of the slopes and slope permeability (Lydia and Espizuajorge, 2002). The most slope shakes after heavy rainfall or melting of snow in spring takes place due to water intrusion in the gaps. Heavy rainstorms induced thousands of Landslides along the Cordillera de la Costa, Vargas, Venezuela and fatalities were estimated to be at least 30,000 (Larsen et al., 2001). The influence of rainfall intensity on the hillslope instability depends on the permeability and other properties of rock masses (Zandi, 1999). The highest rate of precipitation with 32.82% is between 450 and 300 mm. Also, the highest landslide occurred in the same rainfall class (18.21%) and in classes 300–264.8 mm which include 5.90% of the total area of the basin, no slip has been taken.

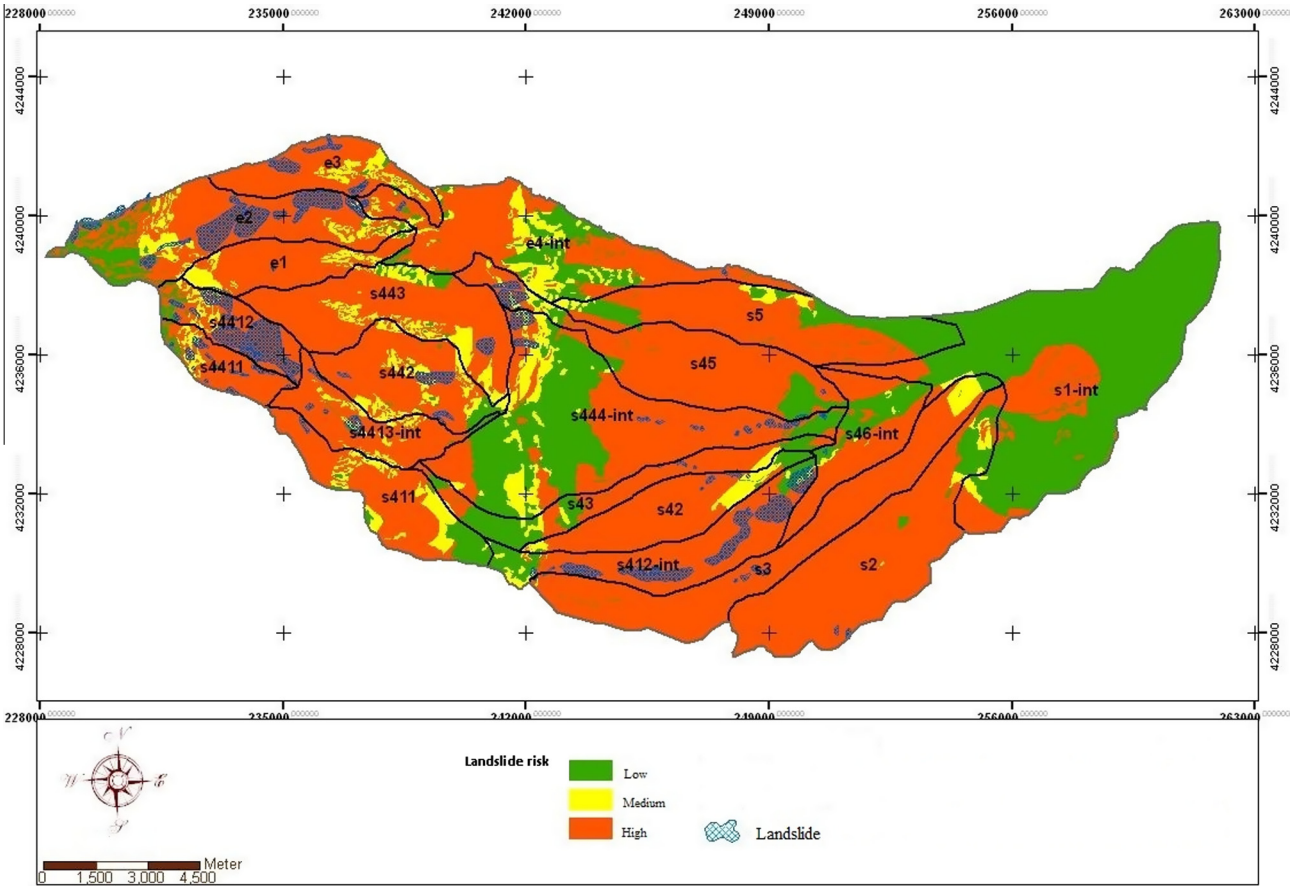

Figure 9 Landslide hazard zoning map.

The results of weighted land use map showed that the lowest landslides occurred in cultivated lands and one of its reasons may be a low slope and gentle topography of the land. About 76% total landslides happened in the range land; therefore, range lands are susceptible to instability. Since the path of potential faults is based on unstable parts of the earth and also due to creating shakes in the layers and infiltration of water into them, cutting resistance decreases in hillslopes (Yaqhubi Shalmani, 2006). The results showed that the highest rate of slips (39.18%) occurred within 500 meters of the faults. Away from the fault, slip rate is reduced. Matthew et al. (2007), during their studies on Himalaya's landslides in India, also found the same result as they attributed most of the landslides occurred near the fault. Further study of landslides in north Beijing by Jingkun and Ruan Qiuqi (1991) also obtained similar results showed that the greatest mass movements occurred in distances lower than 500 meters of the fault (34.5% of basin area). Shadfar et al., 2011 stated that 97% of slides have occurred in distances lower than 2000 m of the fault.

Among the important points is reducing slip in 1000–500 m distance of the fault as compared with landslide rates between 1500 and 1000 m which can be associated with rock genders and slopes because the areas have been covered with basalt and andesite rocks. The results indicated that 50.31% of landslides occurred in andesite and basalt lavas. Despite the high resistance of these rocks, other factors such as high slope of this area, and existing fault, influenced on instability and caused the occurrence of frequent landslides in this region.

5. Conclusion

Pay attention to Table 8, 67.85% basin has a high instability, 7.76% moderate instability and 24.39% low instability. Landslide hazard zoning map of the basin is observed in Fig. 9. Shadfar et al., 2011 computed 63% instability (high landslide risk) by LNRF in the Jalisan basin, Tonekabon, Iran. They estimated that landslide risk exists in 66% and 79% of the basin base on the Information Value Method (IVM) and Density Area (DA), respectively. Akbari and Mashayekhan (2012) compared two models of LNRF and (Weighted Linear Combination) WLC in providing the landslide risk map and concluded that 50 and 71% areas of the basin are unstable with regard to landslide hazard, respectively. In conclusion, we can say that this basin suffers from a relatively high potential of instability to make us largely hesitate to develop the basin for urban and tourism land uses.

Acknowledgments

The authors would like to thank the Islamic Azad University, Rasht Branch, Rasht, Iran, for their aid and the use of equipment and facilities.

References

Akbari, M., Mashayekhan, A., 2012. The comparison of conceptual model LNRF and WLC in zoning landslide risk (case study: Akhlamd basin, Chenaran, Khorasan, Iran). J. Iran. Watershed Manag. Sci. Eng. 6 (18), 1–10 (in Persian).

Aleotti, P., Chowdhury, R., 1999. Landslide hazard assessment: summary review and new perspectives. Bull. Eng. Geol. Environ. 58, 21–44.

Anbalagan, R., 1992. Landslide hazard evaluation and zonation mapping in mountainous terrain. Eng. Geol. 32, 269–277.

Ayalew, L., Yamagishi, H., 2005. The application of GIS-based logistic regression for landslide susceptibility mapping in the Kakuda-Yahiko Mountains, Central Japan. Geomorphology 65, 15–31.

Bouma, N.A., Imeson, A.C., 2000. Investigation of relationships between measured field indicators and erosion processes on badlands surfaces at Petrer, Spain. Catena 40 (2), 147–171.

Busoni, E., Salvador, S.P., Calzolari, C., Romagnoli, A., 1995. Mass movement and erosion hazard patterns by multivariate analysis of landscape integrated data: the upper Orcica river valley (Siena, Italy) case. Catena 25 (1–4), 169–185.

Dai, F.C., Lee, C.F., 2002. Landslide characteristic and slope instability modeling using GIS, Lantau Island, Hongkong. Geomorphology 42, 213–228.

Esmali, A. and Ahmadi. H. 2003. Using GIS and RS in mass movements hazard zonation. A case study in Germichay watershed, Ardabil, Iran. http://www.gisdevelopment.net/application/natural_hazards/landslides/mao3004.htm.

Furuya, G., Sassa, K., Hirua, H., Fukuoka, H., 1999. Mechanism of creep movement caused by landslide activity and underground erosion in crystalline schist, Shikoku Island, southwestern Japan. Eng. Geol. 53 (3–4), 311–325.

Gupta, R.P., Joshi, B.C., 1990. Landslide hazard zoning using the GIS approach, a case study from the Ramanga Catchment Himalayas. Eng. Geol. 28, 119–131.

Gupta, R.P., Saha, A.K., Arora, M.K., Kumar, A., 1999. Landslide hazard zonation in part of Bhagirathi Valley, Garhwal Himalaya, using integrated remote sensing–GIS. Himalayan Geol. 20, 71–85.

Habibi, R., Atarpoor, A., Mirmahmoodi, F., 2005. Investigating efficiency zonation methods of revised Nilsson land slide risk and Taiwan geologists engineering society in the Kan-Sologhan basin. In: The Proceeding 3rd Erosion and Sediment National Conference, September, 2005. Soil Conservation and Watershed Management Research Institute, Tehran, Iran (in Persian).

Haeri, S.M., Samiei, A.H., 1996. New zoning approach of slope areas against the landslide risk with emphasis on zoning of Mazandaran province, Earth Sciences, No. 23 (in Persian).

Haq, M., Akhtar, M., Muhammad, S., Paras, S., 2012. Techniques of remote sensing and GIS for flood monitoring and damage assessment: a case study of Sindh province, Pakistan. Egypt. J. Remote Sens. Space Sci. 15, 135–141.

Hassanzadeh, N.M., 2000. Landslide Hazard Zonation in Shalmanrood Watershed (M.Sc. thesis). Tehran University, Tehran, Iran (in Persian).

Jingkun, W., Ruan Qiuqi, W.A., 1991. Landslide Hazard Remote Sensing Information System, GISdevelopment.net, AARS, ACRS 1991, Agriculture/Vegetation.

Khayyam, M. 1993. Attempt on design of construction state and morphology of Azerbaijan volcanic plateau with an emphasis on volcanic mass of Sabalan, J. Lit. Humanit. University of Tabriz, No. 22 (in Persian).

Khezri, S., Rural, S., Rajai, A., 1385, Zoning and cell analysis of slope instability in the central part of river basin of Zab, J. Soc. Hum. Sci. Geogr., University of Tabriz, No. 22 (in Persian).

Larsen, M.C., Wieczorek, G.F., Eaton, L.S., Torres-Sierra, H., Morgan, B.A., 2001. Venezuelan debris flow and flash flood disaster of 1999 studied. Eos. Trans. Am. Geophys. Union 82 (47), 572–573.

Lydia, E., Espizuajorge, D.B., 2002. Land slide hazard and risk zonation mapping in the Rio Grande Basin, central Andes of Mendoza, Argentina. Mt. Res. Dev. 22 (2), 177–185.

Matthew, J., Jiha, V.K., Rawat, G.S., 2007. Weights of evidence modelling for landslide hazard zonation mapping in part of Bhagirathi Valley, Uttarakhand. Curr. Sci. 92 (5), 628–638.

Mohamed, E.S., Schu, B., Belal, A., 2013. Assessment of environmental hazards in the north western coast-Egypt using RS and GIS. Egypt. J. Remote Sens. Space Sci. 16, 219–229.

Najarjan, R., Mukherjee, A., Roy, A., Khire, M.V., 1998. Temporal remote sensing data and GIS application in landslide hazard zonation of part of western Ghat, India. Int. J. Remote Sens. 19 (4), 573–585.

NRSA, 2001. Landslide hazard zonation mapping along the corridors of the pilgrimage routes in Uttaranchal Himalaya, Technical document, NRSA, Department of Space, India.

Rasmy, M., Gad, A., Abdelsalam, H., Siwailam, M., 2010. A dynamic simulation model of desertification in Egypt. Egypt. J. Remote Sens. Space Sci. 13, 101–111.

Refahi, H.Gh., 2000. Soil Erosion by Water & Conservation, Second ed. Tehran University Publications, 551 p, in Persian.

Sabagh, H., 2009. Detecting the Morphological Evidence of Quaternary Climatic Changes in the Basin (M.Sc. thesis), Islamic Azad University of Ardabil, Ardebil, Iran (in Persian).

Saber, D., 2009. Research in Hydro-clima of Sabalan Basin Block Ardabil Tea with Emphasis on its Role in Creating Erosion and Sedimentation of the Basin (M.Sc. thesis), Islamic Azad University of Ardabil, Ardebil, Iran (in Persian).

Saha, A.K., Gupta, R.P., Arora, M.K., 2002. GIS-based landslide hazard zonation in the Bhagirathi (Ganga) valley, Himalayas. Int. J. Remote Sens. 23, 357–369.

Sassa, K., 1984. Monitoring of a crystalline schist landslide: compressive creep affected by ''underground erosion''. In: Proc. 4th International Symposium on Landslide, Univ. Toronto Press, Toronto, Downsview, vol. 2, pp. 179–184.

Shadfar, S., Norouzi, A.A., Ghodosi, J., Ghayumian, J., 2005. Zoning landslide hazard in the basin of Laktrash. Sci. J. Soil Water Cons. Ext. 1, 1–10 (in Persian).

Shadfar, S., Yamani, M., Namaki, M., 2011. Zoning land slide hazard by Information Value Method (IVM), Density Area (DA) and Landslide Numerical Risk Factor (LNRF) model in Chalkrood. J. Watershed Manage. Eng. 3 (1), 40–47 (in Persian).

Yaqhubi Shalmani, H., 2006. Study the Mass Movements with Emphasis on Climate in Rudbar (M.Sc. thesis), Islamic Azad University-Rasht Branch, Rasht, Iran (in Persian).

Zandi, F., 1999. Investigation of Lineaments in the Region of Taleghan using Remote Sensing and its Application in Identifying Slip Areas (M.Sc. thesis), Shahid Beheshti University, Tehran, Iran (in Persian).